

Behavior of multi-story steel buildings under dynamic column loss scenarios

Seth T. Hoffman¹ and Larry A. Fahnestock^{2*}

¹*Peter Kiewit Sons' Inc., Omaha, NE, USA*

²*University of Illinois at Urbana-Champaign, Urbana, IL, USA*

(Received August 30, 2010, Accepted February 14, 2011)

Abstract. This paper presents a computational study of column loss scenarios for typical multi-story steel buildings with perimeter moment frames and composite steel-concrete floors. Two prototype buildings (three-story and ten-story) were represented using three-dimensional nonlinear finite element models and explicit dynamic analysis was used to simulate instantaneous loss of a first-story column. Twelve individual column loss scenarios were investigated in the three-story building and four in the ten-story building. This study provides insight into: three-dimensional load redistribution patterns; demands on the steel deck, concrete slab, connections and members; and the impact of framing configuration, building height and column loss location. In the dynamic simulations, demands were least severe for perimeter columns within a moment frame, but the structures also exhibited significant load redistribution for interior column loss scenarios that had no moment connectivity. Composite action was observed to be an important load redistribution mechanism following column loss and the concrete slab and steel deck were subjected to high localized stresses as a result of the composite action. In general, the steel buildings that were evaluated in this study demonstrated appreciable robustness.

Keywords: multi-story buildings; steel frames; structural integrity; progressive collapse; connections; composite beams; dynamic response; finite element method.

1. Introduction

The collapses of the World Trade Center Twin Towers in 2001 have generated an extensive focus in the United States on the issues of structural robustness, integrity and collapse resistance. Owing to the uncertainty related to events that could trigger collapse, such as blast or impact loading, and the wide range of methods that can be used to evaluate structural response, study of collapse resistance has spanned a broad spectrum. However, the most common approach for evaluating collapse resistance is the alternate path method that is presented in the United States Department of Defense (DoD) document *Design of Buildings to Resist Progressive Collapse* (DoD 2009). This is classified as a threat-independent approach since it does not define the initiating event but considers loss of a primary structural element and evaluates the ability of the structure to redistribute load around the damaged region. Although the alternate path method uses a simplistic representation of a damaging event, it is a versatile method that allows for a variety of damage scenarios to be examined and compared. The research presented in this

* Corresponding author, Assistant Professor, E-mail: fhnstck@illinois.edu

paper employs the alternate path method to evaluate the dynamic behavior of multi-story steel buildings with perimeter moment frames and composite steel-concrete floors when subjected to various column loss scenarios. This study provides insight into: three-dimensional load redistribution patterns; demands on the steel deck, concrete slab, connections and members; and the impact of framing configuration, building height and lost column location.

Recent research on robustness of steel buildings has focused on a variety of important issues. Khandelwal and El-Tawil (2007) conducted computational simulations of bare steel moment-resisting beam-column connection subassemblies under column loss scenarios and demonstrated the ductility of seismically-designed connections and their ability to deform in catenary mode. Sadek et al (2009) developed computational models and conducted full-scale tests of bare steel moment-resisting beam-column connection subassemblies under column loss scenarios, which demonstrated large monotonic rotation capacity without strength degradation. Sadek et al (2008) and Alashker et al (2010) focused on one-floor two-bay square composite steel-concrete floor system subassemblies with shear connections under column loss scenarios. These studies demonstrated the significant contribution of the floor system to collapse resistance and identified the steel deck as the primary contributor, but also found that the load-carrying capacity is less than specified by progressive collapse guidelines (DoD 2009). Izzuddin et al (2008) developed a simplified framework for progressive collapse assessment of multi-story buildings and demonstrated its applicability through case studies considering perimeter and corner column loss in a typical composite steel-concrete floor system subassembly (Vlassis et al 2008). These macro-model simulations indicate that such floor systems can be prone to progressive collapse and that tying force requirements alone cannot comprehensively ensure structural robustness. Khandelwal et al (2008, 2009) used macro-model simulations to evaluate collapse resistance of seismically-designed steel moment frames and braced frames, and these simulations indicated that system strength and member layout play a larger role than ductile detailing in improving collapse resistance. Several recent studies have employed three-dimensional finite element models to evaluate robustness of steel buildings. Alashker and El-Tawil (2010) compared two-dimensional and three-dimensional simulations of column loss in a ten-story steel building and illustrated the substantial difference between them, largely due to the contribution of the floor system in the three-dimensional model, which created alternate load paths that can reduce the effect of column loss. Kwasniewski (2010) used a detailed finite element model to study collapse behavior of an eight-story steel building, Fu (2009, 2010) used a detailed finite element model to study collapse behavior of a twenty-story steel building, Main and Sadek (2009) used a macro-model to study collapse behavior of a ten-story steel building, and Foley et al (2007) used frame element models to study collapse behavior of three-story, nine-story and twenty-story steel buildings. Krauthammer and Yim (2009) used frame element models that included shell elements to represent the concrete slab to study the effect of simultaneous multiple column loss in a ten-story steel building. Across a range of modeling complexity, these studies concluded that the buildings exhibited robust performance and that there was low potential for progressive collapse. Although the studies conducted to date give important insight into the behavior of steel buildings under column loss scenarios, there are still a wide range of issues remaining to be explored related to the collapse resistance of steel buildings when subjected to severe localized damage. The present study was initiated with the intent of providing new knowledge about three-dimensional steel building response and factors that influence load redistribution and collapse resistance under dynamic column loss scenarios.

2. Prototype buildings and numerical models

For this study, two buildings representative of typical low and mid-rise steel construction in a low seismic region of the United States were selected: the three-story and ten-story Boston pre-Northridge buildings from the SAC suite of prototype buildings (FEMA 2000a). The three-story and ten-story buildings have plan dimensions of 36.6 m × 54.9 m and 45.7 m × 45.7 m as shown in Figures 1(a) and 1(c), respectively. The buildings have interior gravity-only framing with perimeter moment frames for lateral load resistance. Gravity beams and girders are attached with ASTM A36 steel single plate shear connections welded to the supporting member and bolted to the supported member with 19 mm diameter ASTM A325 high strength bolts. Moment frame beams and girders are connected to the columns with welded unreinforced-flange moment connections and single plate shear connections. Elevation views of the three-story and ten-story moment frames are shown in Figures 1(b) and 1(d), respectively. All beams, girders and columns are wide-flange shapes comprised of ASTM A992 steel. The floor system consists of 51 mm corrugated steel deck topped with 76 mm of normal-weight concrete with a compressive strength of 35 MPa. ASTM A615 Grade 60 6 × 6-W1.4 × 1.4 wire mesh is

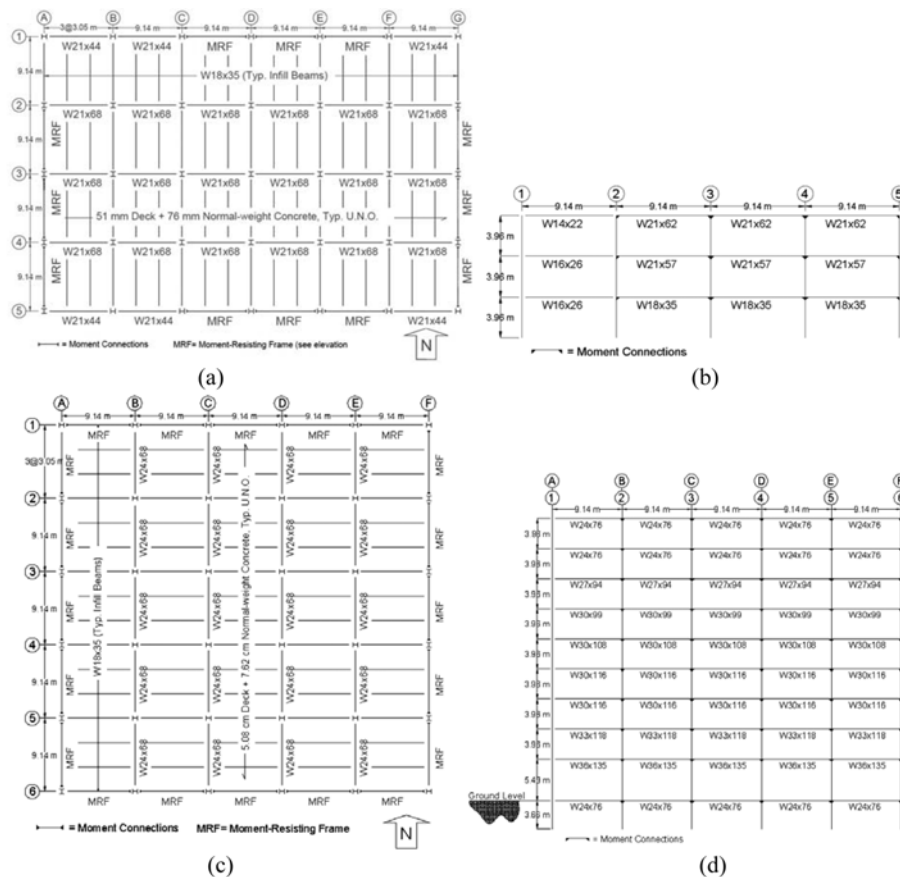


Fig. 1. Prototype building descriptions: (a) three-story plan, (b) three-story elevation, (c) ten-story plan, (d) ten-story elevation

included in the slab. The slab is composite with all beams and girders through 19 mm diameter \times 102 mm long ASTM A108 shear connectors spaced at 305 mm. Applied loadings are typical for office occupancy and include the structural steel and concrete weight, superimposed dead load of 1200 Pa for floor finishes and mechanical/electrical/plumbing systems and 960 Pa for interior partitions. Cladding loads of 1200 Pa are used on the perimeter surface of the building including a 1.1 m parapet wall at the roof. Live loading is 2400 Pa on all floors and the roof.

The prototype structures were modeled using the commercial finite element package Abaqus (Simulia 2010). The wide-flange beams, columns, and girders were modeled using three-node (Abaqus element type S3) and four-node (Abaqus element type S4R) shell elements, which had dimensions in the range of 75 mm to 100 mm. These are general-purpose conventional shell elements that allow transverse shear deformation and consider finite membrane strain and large rotations. The S4R formulation employs reduced integration with hourglass control, and S3 is a degenerated version of S4R. Material nonlinearities were incorporated through the von Mises material model with associated flow rule and steel stress-strain properties were based on experimental data (Fahnestock et al 2006).

The steel deck and concrete slab were modeled using individual planar layers of four-node S4R shell elements. For the steel deck, representative shell element patch models of the actual fluted deck geometry were used to develop an orthotropic constitutive matrix that was implemented in the planar element layer representing the steel deck, which was offset to the centroid of the physical deck location (25 mm above the steel framing). The concrete below the top of the deck flutes was neglected, so an effective thickness of 76 mm was applied to the shell element layer representing the concrete slab, which was offset to the centroid of the area of the concrete above the flutes (89 mm above the steel framing). This idealization is shown in Figure 2. In the steel deck shell elements, three integration points were used through the thickness and in the concrete slab shell elements, five integration points were used through the thickness. The steel reinforcement within the concrete slab was modeled as a smeared isotropic layer. An elastic perfectly-plastic constitutive relationship was used for the steel deck with a yield stress of 207 MPa, which correlated well to the patch test of the physical geometry when analyzed with typical experimental deck material properties. A smeared cracking model was used for the concrete slab with linear-elastic compression behavior and tension-stiffening tensile behavior. Composite action between the steel framing and steel deck and concrete slab was modeled by applying coupling constraints between nodes in the top flanges of the steel framing, the steel deck layer, and the concrete slab layer, effectively tying the three components together. Element sizes were 305 mm for the steel deck and 152 mm for the concrete slab, which were found to be sufficient when a mesh convergence study was conducted. The approach used to model the steel deck and concrete slab is consistent with the techniques employed in other studies of collapse resistance for structures with steel-concrete composite floors (Alashker and El-Tawil 2010, Fu 2009 and 2010, Krauthammer and Yim

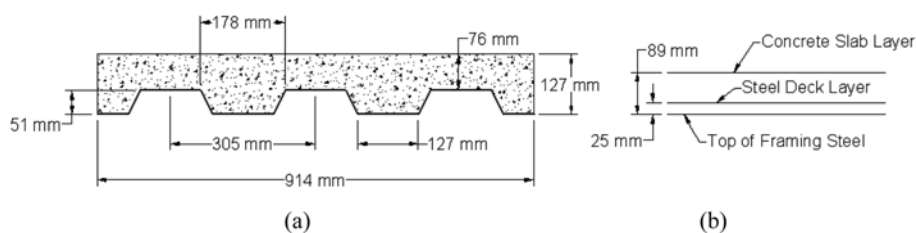


Fig. 2. Steel-concrete composite deck model geometry: (a) physical, (b) model idealization

2009, Kwasniewski 2010, Main and Sadek 2009).

The bolted shear tab connections were represented with a component model consisting of nonlinear springs joining each bolt location on the beam or girder to the supporting member. The configuration for the shear connection model is shown in Figure 3. Bolt tear-out was the governing limit state for the axial capacity of the connections and the force-deformation relationship from Sadek et al (2008) was used. This relationship is shown in Figure 4 for the connection sizes used in the models. After the point of peak strength, further tensile displacement causes a damage variable to increase, which degrades the capacity of the connection up to a failure. In the shear direction, the same force-deformation relationship was applied without degradation. Nonlinear springs with initial gaps were also included between the top and bottom flanges of the beams and the supporting member to account for flange binding. After the 13 mm initial gap in the spring closes, rigid normal contact is modeled between the beam flange and the supporting member. For the welded flange moment connections, the flanges were rigidly connected to the supporting columns by tying coincident nodes in the beams and columns. The bolted shear tab connection model described above was also used within the welded unreinforced flange moment connections.

The finite-element models were constructed with the first-story portion of a single column omitted. At the location of the omitted column, a fixed vertical boundary condition was applied. Loads were introduced by defining appropriate material densities for all structural components and applying superimposed dead and live loads as distributed nonstructural masses to the floor slabs. These accounted for the full dead load and 25% of the live load. The models were then analyzed in two steps

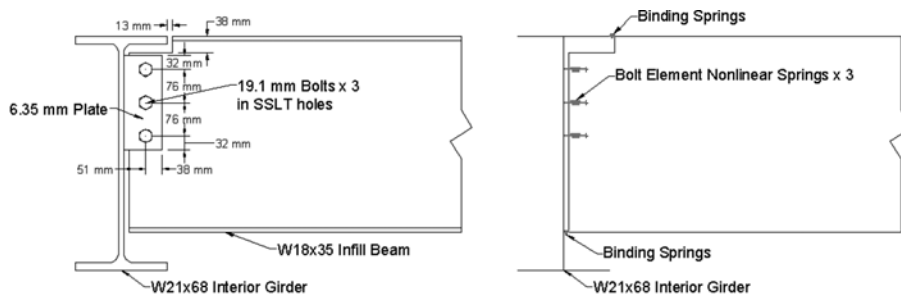


Fig. 3. Bolted shear tab connection model geometry: (a) physical, (b) model idealization

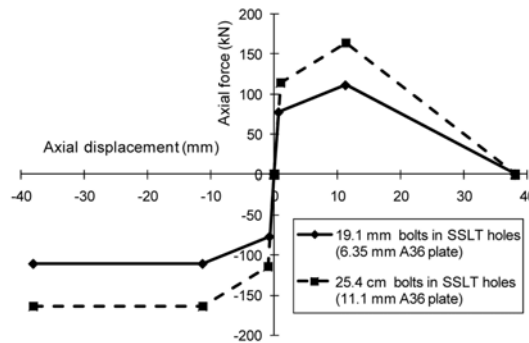


Fig. 4. Shear tab bolt tear-out behavior

employing the Abaqus/Explicit dynamic analysis engine. In the first step, a uniform gravitation field was gradually applied to the entire model over an analysis period of one second to reach the static loading condition. Mass scaling was used to reduce dynamic effects and to decrease the computational time for this analysis step. The internal forces in the model after the first step were validated against static analysis to confirm that the mass scaling parameters were appropriate and did not affect the response. Following gravity load application, the vertical boundary condition at the removed column was turned off instantaneously and the model was run for one second to capture the critical response following column loss.

3. Simulation results

A total of sixteen individual column loss simulations were performed, consisting of twelve for the three-story building and four for the ten-story building. These simulations captured nearly all possible variations of surrounding structural geometry and connectivity in the three-story building and the most significant variations in the ten-story building. Since some critical limit states, such as fracture of the deck, shear connectors, members and connections, are not included in the models, these simulations should not be used primarily to judge collapse or non-collapse, but to make relative comparisons between the various cases. However, the column loss scenarios that led to structural collapse, both in the three-story building, are certainly very vulnerable. Out of the sixteen simulations performed, two are presented first as case studies. Both are from the three-story building and they consist of a perimeter column connected with moment framing on one side and gravity framing on the other, and an interior column connected only with gravity framing. These two simulations did not indicate collapse, but the demands are significant and collapse is not precluded owing to the limitations of the model noted above. The results from all sixteen simulations are then used to study the general behavior and trends following column loss in the three-story and ten-story buildings. Overall system response, load redistribution mechanisms and patterns, and performance of the connections, steel deck and concrete slab are discussed.

3.1 Case studies

3.1.1 Three-story building, column A2 loss

Prior research has shown that multistory steel buildings have the capacity to bridge over the loss of a column within a moment frame (Foley et al 2007, Khandelwal et al 2008), but the response following loss of a perimeter column with moment connections only on one side is less clear. Simulation of Column A2 loss in the three-story building, which is located on the building perimeter with gravity framing on one side and moment framing on the other, provides some insight into this case. Following column loss, the simulation indicates that collapse was arrested with a peak vertical displacement of 610 mm as shown in Table 1 and Figure 5. However collapse is not precluded owing to the limitations of the model noted above. As shown in Figure 6, the displacement distribution was contained within the two compromised panels and largely symmetrical surrounding the lost column, despite the unbalanced framing with moment connections on one side and simple shear connections on the other. Figure 7 illustrates that at column A2 the panel zones, which did not have doubler plates, experienced severe demands and plastic hinge development in the adjacent beams attached with moment connections was

Table 1 Peak vertical displacements at lost column

Building height	Column location	Lost column	Displacement (mm)
Three-story	Corner	A1	NA - collapse
		A5	320
	Perimeter	A2	610
		A3	120
		A4	130
		B1	NA - collapse
		C1	380
		D1	120
	Interior	B2	440
		B3	370
C2		350	
C3		320	
Ten-story	Corner	A1	43
	Perimeter	B1	41
		A2	53
Interior	B2	350	

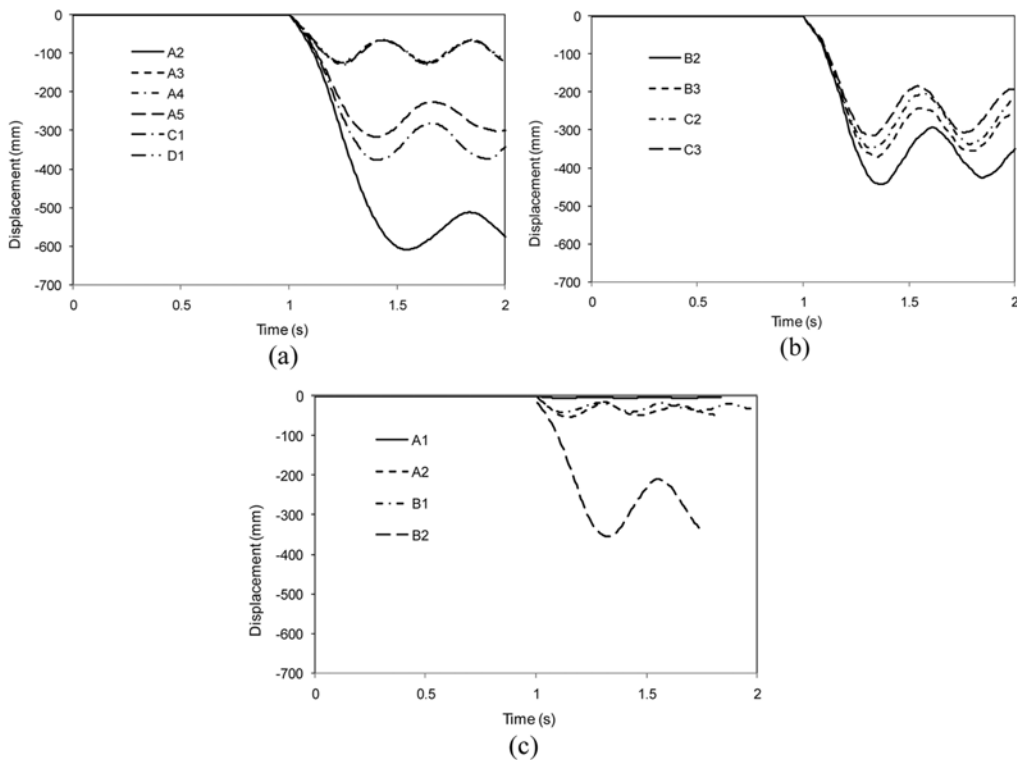


Fig. 5. Vertical displacement at missing column: (a) three-story building perimeter, (b) three-story building interior, (c) ten-story building

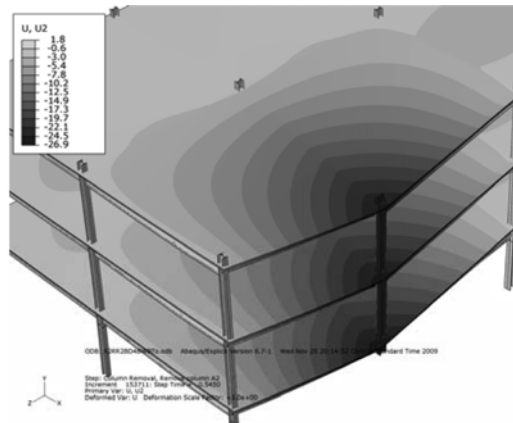


Fig. 6. Displacement contours for Column A2 loss in three-story building (legend shown is in, 1 in = 25.4 mm)

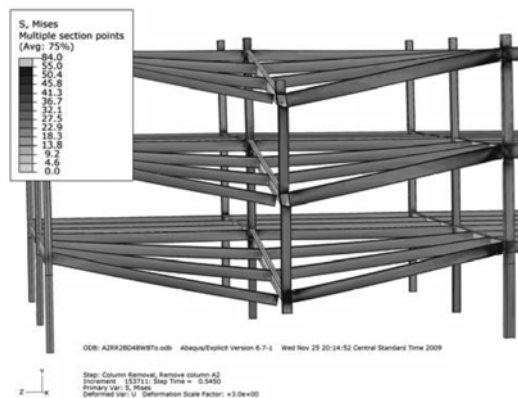


Fig. 7. Effective stress contours for Column A2 loss in three-story building (legend shown is ksi, 1 ksi = 6.895 MPa)

limited. Note that in this figure, the separation shown between the beams and column on the North side of Column A2 indicates significant deformation of the connector elements that represent the shear connections. Away from the lost column near column A3, the beams attached to the column with moment connections developed more pronounced plastic hinges, but lateral-torsional buckling occurred due to compression in the unbraced bottom flange. Although fracture was not directly modeled, the high demands in the moment connections and adjacent panel zones indicate that fracture may occur. The primary load-redistribution mechanism was cantilever action provided by the moment frame along Column Line A. As seen in Figure 8, Column A3 experienced the highest increase in axial force, with a ratio of 2.41 referenced to the force prior to column loss, while the surrounding columns connected by gravity framing showed significantly smaller increases. The Column A1 axial force ratio was 1.79, illustrating the importance of the moment connections compared to the shear connections. However, the force carried by Column A1 illustrates the contribution of positive flexural composite action, where the slab is in compression and the beam is in tension, that developed across the lost column and allowed two-bay single-span redistribution to occur between Columns A1 and A3.

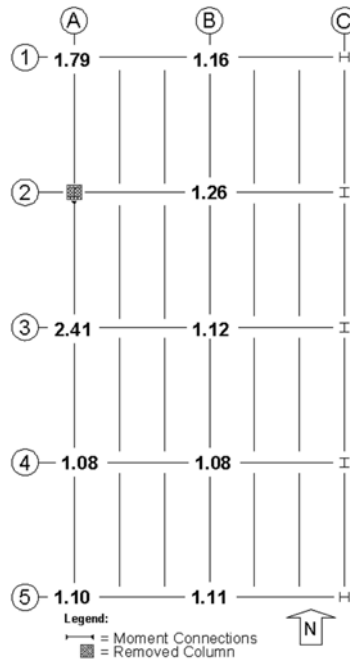


Fig. 8. Column axial force ratios following Column A2 loss in three-story building

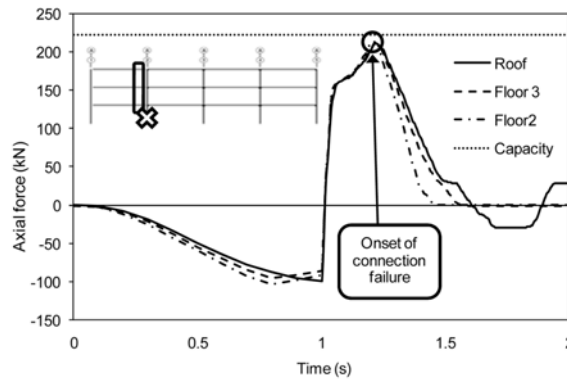


Fig. 9. Shear connection axial forces following Column A2 loss in three-story building

However, the limited axial tensile capacity of the simple shear connections on the north side of Column A2 prevented this from being mobilized to its full potential as the connections reached their peak strength and began degrading prior to peak displacement of the lost column, as illustrated in Figure 9. In a similar manner, the infill beams developed flexural composite action while functioning in a two-bay single-span configuration. As will be demonstrated in more detail below, this behavior is facilitated when the infill beams are oriented parallel to the edge of the building where column loss occurs, but this type of flexural composite action cannot be mobilized when the infill beams are oriented perpendicular to the edge of the building where column loss occurs.

3.1.2 Three-story building, column C3 loss

Prior research related to interior column loss has focused on isolated one-floor two-bay square subassemblies (Sadek et al 2008, Alashker et al 2010), so examination of interior column loss within a full building context is valuable. Interior columns in both the three-story and ten-story buildings did not have adjacent moment frames available for load redistribution, but flexural composite action through the shear connections at the lost column allowed two-bay single-span action to provide the capacity to arrest collapse. Column C3 loss in the three-story building provides the best example of this mechanism, as it represents a full interior condition, with negligible effects from the building perimeter. The peak displacement at the lost column was 320 mm as shown in Figure 5. In the center of the compromised panels at the lost column, significant positive flexural composite action, where the concrete slab was in compression and the steel beams and girders were in tension, developed in both directions of framing across the lost column on all floors. The infill beams in the compromised panels also displayed this behavior in their connections to girders along Column Line 3. An example of the tension force that developed to create the composite flexural action is shown in Figure 10. Although the connections to Column C3 accumulated some damage due to the axial demand, the ductile tear-out limit state provided post-peak capacity and complete connection failure did not occur.

At the perimeter of the compromised panels, some negative flexural composite action was developed through tension in the slab reinforcement and steel deck and compression in the shear connections. An example of the increased axial compressive force is shown in Figure 11. The compressive force reached a peak and declined slightly before the peak displacement was reached due to bottom beam flange binding. This binding effect, illustrated in Figure 12, was beneficial as it introduced additional compressive capacity for mobilizing flexural composite action. The combination of positive flexural composite action through Column C3 Line 3 with the more limited negative flexural composite action at the outside edges of the compromised panels allowed load to be redistributed to adjacent intact columns. As Figure 13 shows, the directly-connected columns experienced the highest peak force increases, with column axial force ratios ranging from roughly 1.5 to 1.75. Columns C2 and C4 participated most significantly in force redistribution due to two-bay single-span action of the infill beams in the affected panels carrying load into girders along Column Lines 2 and 4. This load path also resulted in the columns at the corners of the four affected panels (Columns B2, B4, D2 and D4) carrying increased loads.

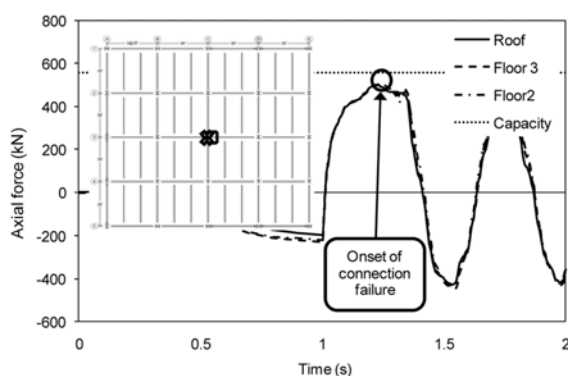


Fig. 10. Shear connection axial forces at Column C3 following Column C3 loss in three-story building

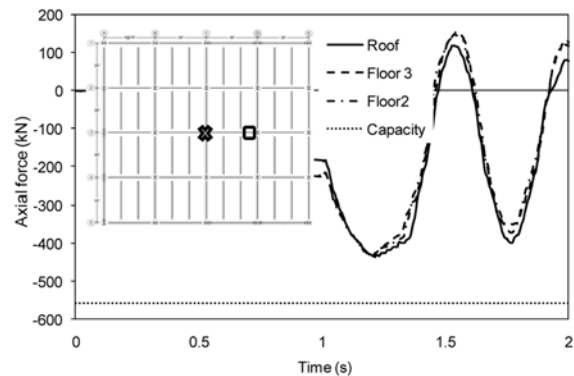


Fig. 11. Shear connection axial forces at Column D3 following Column C3 loss in three-story building

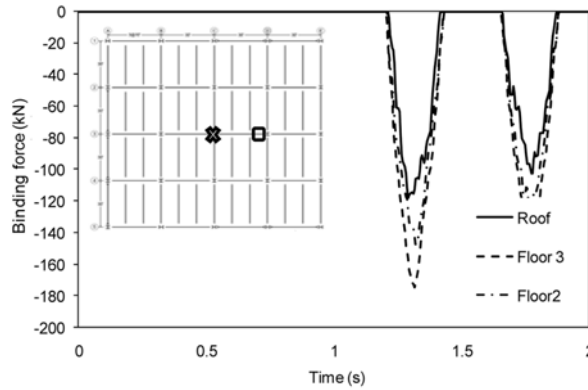


Fig. 12. Shear connection bottom flange binding forces at Column D3 following Column C3 loss in three-story building

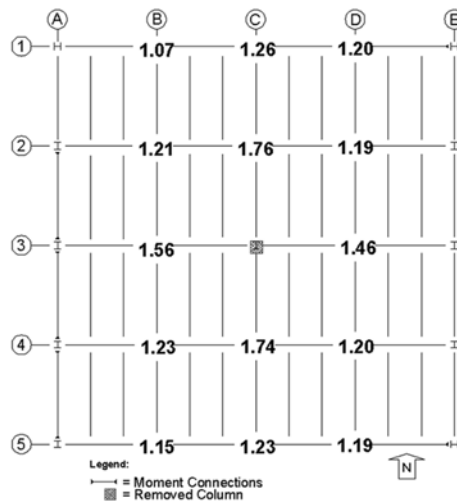


Fig. 13. Column axial force ratios following Column C3 loss in three-story building

3.2 Overall behavior and trends

3.2.1 System response

Of the sixteen column loss scenarios considered in this research, only loss of Columns A1 and B1 in the three-story building resulted in collapse. As noted above, since some critical limit states, such as fracture of the steel deck, shear connectors, members and connections, are not considered in the models, collapse prevention in the other cases is not assured, but the two collapse scenarios are clearly the worst cases. The key difference between the two cases that led to collapse and the remaining cases was the surrounding connectivity. Both Columns A1 and B1 were located on the building perimeter (and Column A1 is at the corner of the building) with no moment connections to the compromised column. All other corner and perimeter column locations analyzed in both buildings had moment connections on at least one side. The interior column loss scenarios that were examined did not have the

benefit of moment connections, but the additional framing continuity in the two orthogonal in-plane directions provided bridging capacity through flexural composite action.

As shown in Table 1 and Figure 5, the peak vertical displacements at the compromised column for scenarios that did not collapse varied widely, from less than 50 mm to over 600 mm. In the three-story building, loss of a perimeter column with a moment frame on one side and gravity frame on the other (Columns A2 and C1) led to the highest peak displacement. The loss of a corner column with one adjacent moment frame (Column A5) resulted in smaller peak displacements, and the loss of perimeter columns with moment frames on both sides (Columns A3, A4, and D1) resulted in the smallest peak displacements. Lost interior columns exhibited more consistent peak displacements, which were in the 300 mm to 460 mm range. In the ten-story building, the corner and perimeter column locations (Columns A1, A2 and B1) exhibited similar peak displacements, around 50 mm, which is much smaller than for similar locations in the three-story building. However, the loss of an interior column in the ten-story building led to similar displacements as observed for interior column loss in the three-story building.

The number of stories in the building subjected to column loss did not appreciably affect the performance. Although the ten-story building behaved much more favorably for corner and perimeter column loss scenarios, this was due to the much larger moment frame members, which were required for lateral load resistance, not the number of stories in the building. Each floor primarily redistributed its own loads from the compromised region out to surrounding intact columns and there was little redistribution up or down the building. This conclusion is illustrated by comparing the interior column loss scenarios between the three-story and ten-story buildings and noting that they are essentially the same.

The first peak of vertical displacement at the lost column typically represented the point of maximum structural demand on the system. In the following discussions of structural capacity and behavior, the maximum values from the entire analysis are used, but these generally occurred at the time of first peak displacement. Response and demands for a single column loss were essentially the same for all floors in the structures, so behavior will be discussed using averages across all individual floors.

3.2.2 Load redistribution

The dominant load redistribution mechanism that was observed in nearly all column loss scenarios was flexural composite action. Both positive and negative flexural composite action developed during column loss, but positive flexural composite action was more significant. Flexural composite action was the only appreciable load-redistribution mechanism mobilized through simple shear connections, but it was also significant in moment connections, particularly in positive flexure. For the cases of corner column loss, flexural composite action was observed, but flexural capacity within the moment connections was the dominant load-transfer mechanism. Positive flexural composite action developed through a force couple with compression in the concrete slab and tension in the steel framing, which was transferred through the remaining portion of the lost column via the beam-column connections. In negative flexure, the sign of the force couple was reversed. Since the concrete slab did not carry significant tension, the tension side of the negative moment couple was provided by the steel deck and the welded wire mesh in the slab, with the former contributing most significantly.

To quantify and compare flexural composite action in a simple manner, composite moment indices were calculated. For positive flexure, a moment was calculated based on the tensile force in the steel connection acting at the centroid of the connection and the compressive force acting at the centroid of the portion of the slab above the top of the deck flutes. For negative flexure, a moment was calculated based on the compressive force acting at the centroid of the steel connection and the tensile force acting

at the centroid of the steel deck. In both cases, these moments were normalized by the plastic moment capacity of the associated steel framing to provide composite moment indices that demonstrate the relative contribution of flexural composite action. Although negative composite moment can be affected by bottom flange binding, for more straightforward comparison, this behavior was neglected when calculating the composite moment indices. The aggregate composite moment indices discussed below are average values over the height of the building at the noted locations.

For non-corner perimeter and interior column loss cases, positive flexural composite action allowed load redistribution by providing a two-bay single span across the compromised column location. As shown in Figure 14(a), the highest composite moments were mobilized through the lost column for perimeter column loss cases in the three-story building with moment frames on both sides (Columns A3 and D1). In these cases, the composite moment indices were around 0.8. Moment connection axial forces are plotted in Figure 15 for the Column A3 loss scenario. Despite experiencing larger peak displacements, as shown in Table 1, loss of Columns A2 and C1 mobilized much smaller composite moments through the lost column. These columns were located at the ends of moment frames and had gravity framing on the opposite side, so the simple shear connections were unable to develop the same axial capacity as the welded moment connections. This resulted in composite moment indices around 0.15. The two perimeter column-loss cases in the ten-story building had moment frames on both sides

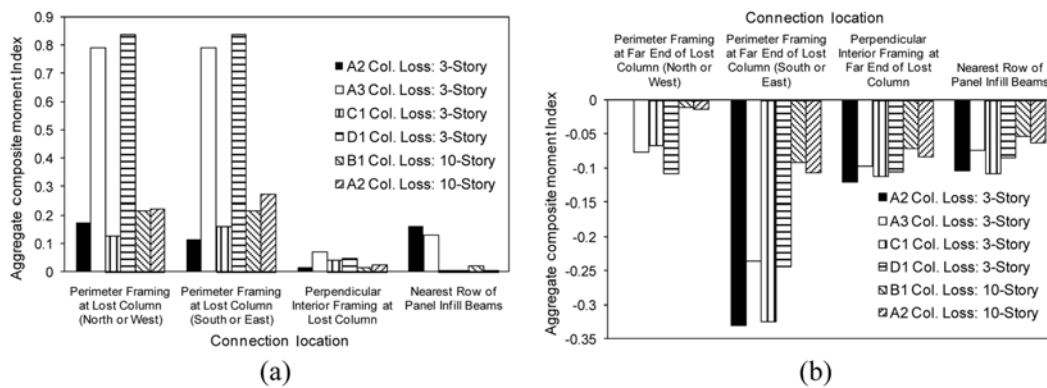


Fig. 14. Aggregate composite moment indices: (a) positive moment, (b) negative moment

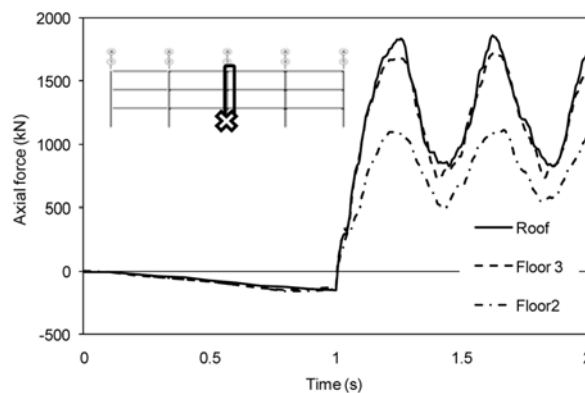


Fig. 15. Moment connection axial forces at Column A3 following Column A3 loss in three-story building

of the lost column, but the composite moment indices were only about 0.20, as the much larger beam sections (relative to the three-story building) significantly reduced peak displacements and carried more moment in the steel beam sections.

The perpendicular gravity framing at the lost column also developed some positive-bending moment, as seen in Figure 14(a), but the composite moment indices were less than 0.1 due to the lack of continuity at the edge of the building. For removal of Columns A2 and A3 in the three-story building, the first row of infill beams, parallel to the building perimeter, also developed composite flexural capacity, due to two-bay single-span action, with composite moment indices around 0.15. In the three-story building, the column removal scenarios (Columns B1 and C1) with infill beams oriented perpendicular to the building perimeter developed negligible composite action since the two-bay single-span condition was not present. In the 10-story building, little variation was noted based on orientation of infill beams since the vertical displacements were limited and there was little opportunity for composite action to be mobilized. These trends indicate that, particularly for low-rise buildings, infill beams oriented parallel to the edge of a building provide greater robustness and more opportunity for load redistribution.

At locations away from the perimeter lost columns, negative composite moments also developed, as shown in Figure 14(b). This mechanism was limited by the tensile strength of the steel deck and the welded wire mesh reinforcement in the concrete slab, but composite moment indices between 0.05 and 0.1 were typically observed with the largest values around 0.3. In interior column-loss scenarios for both the three-story and ten-story buildings, the peak positive composite moment indices were approximately 0.16 for both directions of framing at the lost column as well as the closest row of panel infill beams. The negative composite moment indices for interior column-loss scenarios in both buildings were consistently just above 0.10 for connections at the far end of both directions of framing to the lost column as well as at the far ends of the nearest rows of panel infill beams.

The pattern of load redistribution varied considerably depending on the location of the lost column and the configuration of the structure surrounding it. The largest load increases were seen in the adjacent columns that were directly connected to the lost column by framing members, whereas the columns in the corners of the compromised panels saw much smaller load increases. This pattern was consistent for corner, perimeter and interior column loss scenarios. The load redistributed to adjacent columns varied based on the connection types. As expected, columns with beams attached by moment connections saw higher loads than those connected only with shear connections. Figure 16 plots

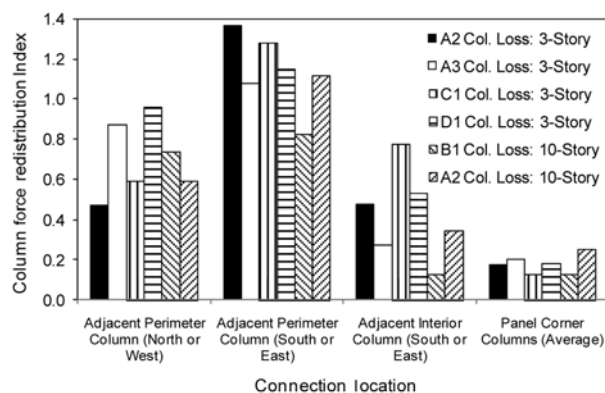


Fig. 16. Column force redistribution index for intact columns adjacent to lost column

column force redistribution index, which is defined as the change in force for an individual column adjacent to a lost column, normalized by the force that had been carried by the lost column. For perimeter column-loss cases, the adjacent columns in the moment frames (South or East) carried the most redistributed force, with redistribution indices typically greater than 1.0. Smaller forces were transferred into the adjacent perimeter column in the North or West direction, as they were either connected to the lost column with only gravity framing, or did not have continuing moment framing on the opposing side of the column to provide additional rotational stiffness as the adjacent South or East columns did. The adjacent interior columns had redistribution indices ranging from 0.1 to over 0.7. For columns at the outlying corners of the compromised panels, load redistribution was smaller, with redistribution indices ranging from 0.1 to 0.2. This redistribution was facilitated by slab two-way action and by the panel infill beams carrying load into girders at the edges of the compromised panels, which then carried the load into the corner columns.

3.2.3 Local demands

The composite floor system composed of steel deck and concrete slab contributed significantly to the alternate load paths following column loss, and as a result these components experienced appreciable demands. For the corner and perimeter column loss scenarios in the ten-story building, the steel deck remained elastic, but in all other column loss cases inelastic response was observed. The yielded regions were generally concentrated around the lost column and the adjacent intact columns, as Figure 17 illustrates for Column A2 loss. In cases where the peak column displacement was large, the deck also yielded above panel infill beams. Since localized failure of the deck at interfaces between sheets was not considered in this research, future work should investigate the capacity of steel deck splices and the effect that these local details have on performance following column loss in light of the contribution that the deck makes to force redistribution. The concrete slab contributed compressive capacity for positive flexural composite action in nearly all column loss scenarios. This resulted in significant compressive demand that exceeded the crushing strength of the concrete in some cases. Only perimeter column loss scenarios with moment framing on one side of the lost column and interior column loss scenarios experienced concrete crushing. The regions subjected to high concrete compressive stress were concentrated above connections where positive flexural composite action had developed, primarily at the lost column, but also at nearby panel infill beam connections. The typical behavior is

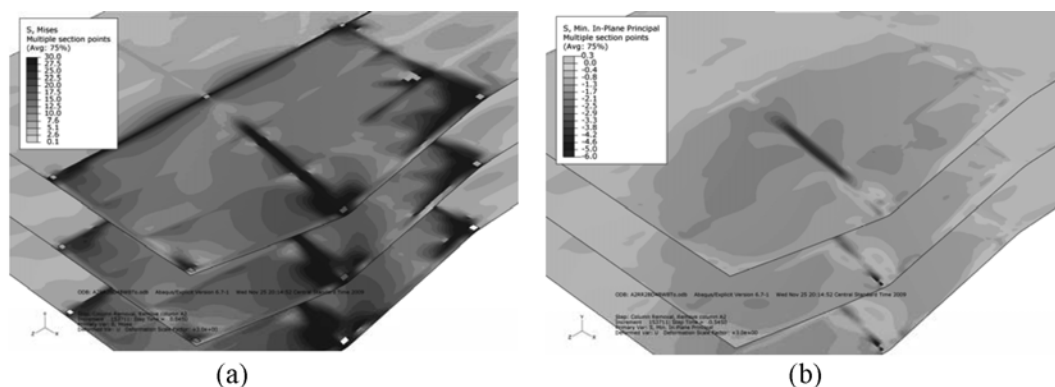


Fig. 17. Von Mises stress contours for A2 column loss: (a) steel deck, (b) concrete slab (legend shown is ksi, 1 ksi = 6.895 MPa)

shown in Figure 17 for the case of Column A2 loss. Although the material constitutive relationship for the concrete slab was linear elastic in compression and did not model the crushing and subsequent degradation in strength, the effect of crushing is judged to be minimal since the regions of crushing were small.

For corner and perimeter column locations, moment connections were critical to successful force redistribution following column loss. In the ten-story building, moment connections remained in the elastic range for all column loss scenarios, so the perimeter column loss scenarios for the three-story building best illustrate moment connection demands including significant inelastic response, and the three-story building will be used in the discussion below. Since the concrete slab provided significant additional compressive axial capacity for connections in positive flexure and the steel deck and slab reinforcing mesh provided some additional tensile capacity for connections in negative flexure, the bottom flanges of the moment connections consistently had higher demands than the top flanges. Aggregate flange yield indices, which are maximum flange forces averaged over the three floor levels for a given location and normalized by the flange yield forces, are presented in Figure 18. These data show that the top flanges only exceeded yield for the loss of Columns A2 and C1, while all column loss scenarios had beam bottom flanges that were loaded into the inelastic range. The large inelastic demands are of concern since they may lead to connection fracture (FEMA 2000b). While significant research has been conducted on welded moment connections for seismic loading (FEMA 2000a, 2000b), limited experimental investigation has been conducted for the distinctly different demands that arise following column loss. Several research programs have studied moment connections under simulated column loss scenarios (Khandelwal and El-Tawil 2007, Sadek et al 2008), but the effect of the composite slab has not been fully explored. As the results of the column loss simulations in this research have demonstrated, flexural composite action appreciably changes the behavior of the moment connections, and the implications of this behavior require additional investigation.

As discussed above, shear connections can play an important role in collapse resistance, primarily by working in conjunction with the concrete slab to mobilize flexural composite action. However, the appreciable demands that are placed on shear connections following column loss can cause localized damage and failure. In the ten-story building perimeter column loss cases, all shear connections remained in the elastic range since the large moment frames effectively redistributed the load from the lost column and limited the vertical deflection. In the three-story building perimeter column loss cases, the moment frames had much smaller members and as a result the shear connections experienced much

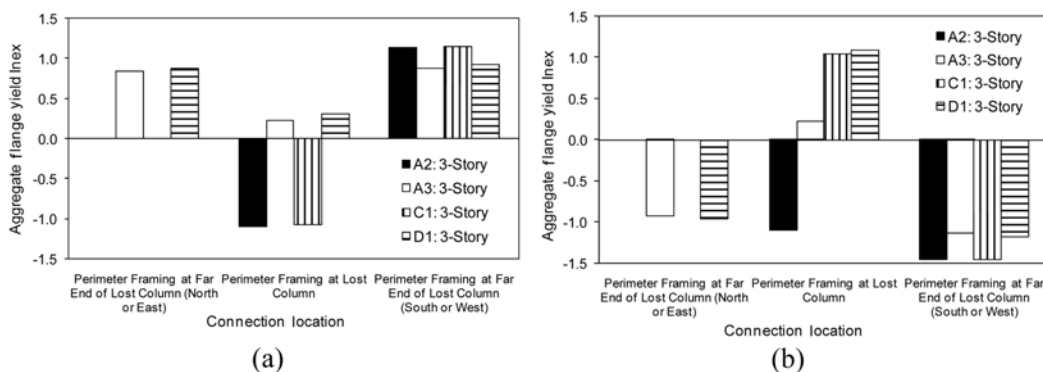


Fig. 18. Aggregate flange yield indices: (a) top flanges, (b) bottom flanges

Table 2 Shear connection demands for three-story perimeter column loss scenarios

Lost Col.	Connection location*			
	Perimeter at far end of lost column (North or East)	Perimeter at lost column	Perpendicular interior at far end of lost column	Perpendicular interior at lost column
A2	-	Axial	-	-
A3	NA - moment conn.	NA - moment conn.	-	-
C1	Shear	Axial	Shear	-
D1	NA - moment conn.	NA - moment conn.	Shear	-

*Axial = axial capacity of connection reached; Shear = shear capacity of connection reached

Table 3 Shear connection demands for interior column loss scenarios

Building height	Lost col.	Connection location*				
		Girder at lost column	Infill beam at far end of lost column (North)	Infill beam at lost column	Infill beam at far end of lost column (South)	Nearest infill beams
Three-Story	B2	Axial	-	Axial, Shear	Shear	Axial
	B3	Axial	Shear	Axial, Shear	Shear	-
	C2	Axial	-	-	Shear	-
	C3	Axial	-	-	Shear	-
Ten-Story	B2	Axial	-	Axial, Shear	Shear	-

*Axial = axial capacity of connection reached; Shear = shear capacity of connection reached

larger demands. Table 2 summarizes the shear connection performance for the four primary perimeter column loss cases (Columns A2, A3, C1 and D1) in the three-story building by noting the connection locations where the modeled axial and/or shear capacities of the connections were reached. Of these four cases, Column A3 loss led to the smallest demands on the shear connections and they remained essentially elastic due to the moment frame action and the favorable orientation of the infill beams (parallel to the building perimeter). In comparison, Column D1 loss, which is similar to Column A3 except the infill beams are oriented perpendicular to the building perimeter, led to shear damage in the connection at the far end of the infill beam that was attached to the lost column. This difference further illustrates the variation in behavior associated with the orientation of infill framing, which was noted above. Similarly, comparison of the loss scenarios for Columns A2 and C1, where the primary difference is infill framing orientation, reveals significantly more inelastic connection response for the Column C1 scenario owing to the infill framing being oriented perpendicular to the building perimeter. Table 3 summarizes the shear connection performance for the interior column loss cases and illustrates the increase in demand on the shear connections due to the lack of moment connections. In all cases, multiple shear connections reached axial and shear capacity and exhibited inelastic response, and the three-story and ten-story buildings behaved similarly. In the three-story building, the loss scenarios for Columns C2 and C3 exhibited the least number of connections with inelastic response since they were further away from the building perimeter and had the benefit of additional slab continuity.

4. Summary and conclusions

Dynamic column loss simulations were conducted for three-story and ten-story prototype steel

buildings with perimeter moment frames and composite steel-concrete floors. Sixteen column loss scenarios were considered and the results from these simulations provide the following key conclusions:

- Corner and perimeter column loss scenarios with only shear connections led to localized collapse, although propagation through the remaining intact portion of the building did not occur.
- Composite flexural response was a significant load redistribution mechanism following column loss. This was most prevalent at the lost column, where connection axial capacity allowed positive flexural composite action to develop. This composite action allowed two adjacent beam spans to act as one span over two bays. Negative flexural composite action also developed at intact columns adjacent to the compromised column.
- The concrete slab and steel deck were subjected to inelastic demands as a result of flexural composite action. For interior column loss scenarios where positive flexural composite action was mobilized, small regions of the concrete slab were loaded to crushing. In most column loss cases, the steel deck was loaded beyond yield. The deck was modeled as continuous, so it did not capture possible damage or failure of splices. Future research should evaluate the impact of failure modes at deck splices.
- For interior column loss scenarios, load redistribution to adjacent columns was roughly 50% greater for intact columns connected to the compromised column by beams when compared to intact columns connected to the compromised column by girders. This was a result of the two-bay single span created by the panel infill beams, which carried load away from the girders in the center of the compromised panels to girders on the perimeter of the compromised two bay square region. Similarly, for perimeter column loss scenarios, more favorable performance was observed when the infill beams were oriented parallel to the adjacent edge of the building.
- Moment connections to a compromised column and to adjacent intact columns experienced significant flexural and axial demands. Moment connection flanges also experienced appreciable localized shear and moment, in addition to the axial forces. Owing to the appreciable impact that composite action has on the behavior of moment connections under column loss scenarios, the implications of this behavior require additional investigation.
- Shear connections were subjected to significant demands following column loss and many were damaged due to large axial forces. Positive flexural composite action mobilized high tensile forces in shear connections, which often led to some degree of bolt tear-out damage in the connections. This was the cause of one of the two collapse scenarios when the shear connections on one side of the lost column failed entirely. In most cases where flexural composite action placed large axial demands on shear connections, damage occurred but degradation was limited. Compressive forces developed in shear connections where negative flexural composite action was mobilized. However, these forces never exceeded the connection capacity since lower-flange binding occurred between the beam and the supporting element, which isolated the shear connection from further compression. Owing to the significant load redistribution following column loss, shear demand exceeded the design capacity for some shear connections, particularly at infill beams connecting an intact column to a lost interior column.
- Building height does not significantly alter behavior following column loss. Response following interior column loss was essentially the same for the three-story and ten-story buildings. Demands for corner and perimeter column loss scenarios were significantly smaller for the ten-story building when compared to the three-story building, but this trend was not due to the building height, but rather due to the much larger moment framing in the ten-story building. Thus, it can be concluded

for the framing configurations that were studied, each floor acted independently to redistribute its gravity load.

- Overall, this study indicates that multi-story steel buildings with perimeter moment frames and composite steel-concrete floors have appreciable robustness and may potentially be capable of arresting collapse in column loss scenarios. However, large demands on the connections, steel deck and concrete slab indicate potential for localized failure modes that are challenging to capture in computational models. Large-scale experimental investigations are needed to explore the complex three-dimensional load redistribution and localized demands that arise following column loss.

Acknowledgements

This research was partially funded by the American Institute of Steel Construction. The computational simulations described herein were conducted using an allocation through the TeraGrid Advanced Support Program. All opinions, findings, and conclusions expressed are those of the authors.

References

- Alashker, Y., El-Tawil, S. and Sadek, F. (2010), "Progressive collapse resistance of steel-concrete composite floors," *J. Struct. Eng.*, **136**(10), 1187-1196, 10.1061/(ASCE)ST.1943-541X.0000230.
- Alashker, Y. and El-Tawil, S. (2010), "Robustness of steel buildings: 3-D modeling, simulation and evaluation." *Proc., ASCE Struct. Cong.* Orlando, FL.
- DoD (2009), "Design of buildings to resist progressive collapse: UFC 4-023-03," United States Department of Defense. Washington, DC.
- Fahnestock, L.A., Sause, R. and Ricles, J.M. (2006), "Analytical and large-scale experimental studies of earthquake-resistant buckling-restrained braced frame systems," ATLSS Report No. 06-01. Lehigh University, Bethlehem, PA.
- FEMA (2000a), State of the Art Report on Systems Performance of Steel Moment Frames Subject to Earthquake Ground Shaking: FEMA-355C. Federal Emergency Management Agency. Washington, DC.
- FEMA (2000b), State of the Art Report on Connection Performance: FEMA 355D. Federal Emergency Management Agency, Washington, DC.
- Foley, C.M., Martin, K. and Scheenman, C. (2007), "Robustness in structural steel framing systems," Report No. MU-CEEN-SE-07-01, Marquette University, Milwaukee, WI.
- Fu, F. (2009), "Progressive collapse analysis of high-rise building with 3-D finite element modeling method," *J. Const. Steel. Res.*, **65**(6), 2369-1278.
- Fu, F. (2010), "3-D nonlinear dynamic progressive collapse analysis of multi-storey steel composite frame buildings," Parametric study. *Eng. Struct.*, **32**, 3974-3980.
- Izzuddin, B.A., Vlassis, A.G., Elghazouli, A.Y. and Nethercot, D.A. (2008), "Progressive collapse of multi-storey buildings due to sudden column loss - Part I: Simplified assessment framework." *Eng. Struct.*, **30**, 1308-1318.
- Khandelwal, K. and El-Tawil, S. (2007) "Collapse behavior of steel special moment resisting frame connections." *J. Struct. Eng.*, ASCE, **134**(5), 646-655.
- Khandelwal, K., El-Tawil, S., Kunnath, S.K. and Lew, S.H. (2008), "Macromodel-based simulation of progressive collapse: steel frame structures." *J. Struct. Eng.*, ASCE, **134**(7), 1070-1078.
- Khandelwal, K., El-Tawil, S. and Sadek, F. (2009), "Progressive collapse analysis of seismically designed steel braced frames." *J. Const. Steel. Res.*, **65**, 699-708.
- Krauthammer, T, Yim, H.C. (2009), "Localized damage effects on building robustness." *Proceedings, ASCE Struct. Cong.* Austin, TX.
- Kwasniewski, L. (2010), "Nonlinear dynamic simulations of progressive collapse for a multistory building." *Eng.*

- Struct.*, **32**, 1223-1235.
- Main, J.A. and Sadek, F. (2009), "Development of 3D models of steel moment-frame buildings for assessment of robustness and progressive collapse vulnerability." *Proceedings, ASCE Structures Congress 2009*, Austin, TX.
- Sadek, F., El-Tawil, S. and Lew, H.S. (2008), "Robustness of composite floor systems with shear connections: modeling, simulation, and evaluation." *J. Struct. Eng.*, ASCE, **134(11)**, 1717-1725.
- Sadek, F., Main, J.A. and Lew, H.S. (2009), "Testing and analysis of steel beam-column assemblies under column-removal scenarios." *Proceedings, ASCE Structures Congress*, Austin, TX.
- Simulia (2010), Abaqus FEA.
- Vlassis, A.G., Izzuddin, B.A., Elghazouli, A.Y. and Nethercot, D.A. (2008), "Progressive collapse of multi-storey buildings due to sudden column loss- Part II: Application." *Eng. Struct.*, **30(5)**, 1424-1438.

CC